Neuron, Vol. 23, 257–271, June, 1999, Copyright ©1999 by Cell Press

Doublecortin Is a Microtubule-Associated Protein and Is Expressed Widely by Migrating Neurons

Joseph G. Gleeson,*† Peter T. Lin,*
Lisa A. Flanagan,‡ and Christopher A. Walsh*§
*Division of Neurogenetics
Department of Neurology
Beth Israel Deaconess Medical Center
Harvard Institutes of Medicine
†Department of Neurology
Children's Hospital
‡Department of Medicine
Brigham and Women's Hospital
Boston, Massachusetts 02115

Summary

Doublecortin (DCX) is required for normal migration of neurons into the cerebral cortex, since mutations in the human gene cause a disruption of cortical neuronal migration. To date, little is known about the distribution of DCX protein or its function. Here, we demonstrate that DCX is expressed in migrating neurons throughout the central and peripheral nervous system during embryonic and postnatal development. DCX protein localization overlaps with microtubules in cultured primary cortical neurons, and this overlapping expression is disrupted by microtubule depolymerization. DCX coassembles with brain microtubules, and recombinant DCX stimulates the polymerization of purified tubulin. Finally, overexpression of DCX in heterologous cells leads to a dramatic microtubule phenotype that is resistant to depolymerization. Therefore, DCX likely directs neuronal migration by regulating the organization and stability of microtubules.

Introduction

Migrating neurons display complex morphological changes during their migration. Time-lapse imaging of migrating neurons (Edmondson and Hatten, 1987; Liesi, 1992; O'Rourke et al., 1992) demonstrates that migration can be divided into two distinct phases: process outgrowth and nuclear/somal translocation. Migration consists of alternation between these two phases, which do not appear to be synchronized with one another (Edmondson and Hatten, 1987; Rivas and Hatten, 1995). During migration, the leading process extends away from, and then retracts toward, the cell soma in an accordion-like fashion over a period of minutes or hours. Rapid extension and retraction of lamellipodia is common, as the leading process takes on a ruffled appearance. After the leading process advances rapidly with little cell body movement, the soma lurches forward in a saltatory fashion (O'Rourke et al., 1992). Although these two types of movements must require extensive cytoskeletal reorganization, the mechanisms controlling these reorganizations are not well understood.

§To whom correspondence should be addressed (e-mail: cwalsh@caregroup.harvard.edu).

Neurons migrating either along radial glia or independent of radial glia demonstrate a variety of cytoskeletal changes within the soma and processes that may underlie these morphological alterations. Actin, neurofilaments, and microtubules are dynamically changing structures in neurons and appear to have adopted novel regulatory mechanisms to solve the unusual morphological challenges that neurons face. In developing neurons, unique anatomic structures include the specialized filamentous interstitial junction along the interface of migrating neurons and glial fibers (Gregory et al., 1988), the specific orientation of microtubules in the growing axon (Baas et al., 1988), and specialized desmosomes (punctae adherentia) along the length of the leading process (Gregory et al., 1988). Furthermore, several cytoskeletal proteins are neuron specific (reviewed by Sullivan, 1988; Julien and Mushynski, 1998), and even the common cytoskeletal proteins appear to have unique ultrastructural localization (Baas and Joshi, 1992) and properties in neurons (Morris and Lasek, 1982; Black et al., 1984), suggesting that novel molecular signals may guide these cytoskeletal alterations.

The identification of genes from human diseases and mouse mutants with defects in neuronal migration may shed light on the pathways regulating these cytoskeletal alterations. Within the last few years, the genes for several human disorders of neuronal migration have been identified, including Miller-Dieker lissencephaly (*LIS1*) (Reiner et al., 1993) and X-linked lissencephaly/double cortex syndrome (des Portes et al., 1998; Gleeson et al., 1998). X-linked lissencephaly and double cortex syndrome are distinguishable X-linked allelic disorders due to a defect in the novel gene *doublecortin* (gene, *DCX*; protein, DCX). In X-linked lissencephaly, seen in males with *DCX* mutations, cortical neuronal migration is severely disrupted, leading to a rudimentary four-layered cortex (Berg et al., 1998). Mutations in *DCX* in heterozygous females lead to a less severe disease, double cortex, in which some neurons form a relatively normal cortex, while a second population of neurons apparently arrests, leading to a collection of neurons beneath the cortex. Since the normal process of X inactivation leads to affected females who are mosaic for neurons expressing either a normal or a mutant copy of *DCX*, one model suggests that neurons expressing the mutant *DCX* allele arrest beneath the cortex (Gleeson and Walsh, 1997). According to this model, mutations in *DCX* lead to a cell-autonomous defect in cortical neuronal migration.

Here, we demonstrate that DCX is expressed widely in migrating neurons throughout the developing and adult nervous system, by neurons that appear to be migrating both radially and nonradially, suggesting it may play a cell-autonomous role in neuronal migration both in and outside of the cortex. DCX localization overlaps with microtubules in cultured cortical neurons, and this relationship is disrupted by colchicine, a microtubule-depolymerizing agent. Furthermore, DCX coassembles with microtubules from brain, and recombinant DCX enhances the polymerization of purified tubulin, apparently

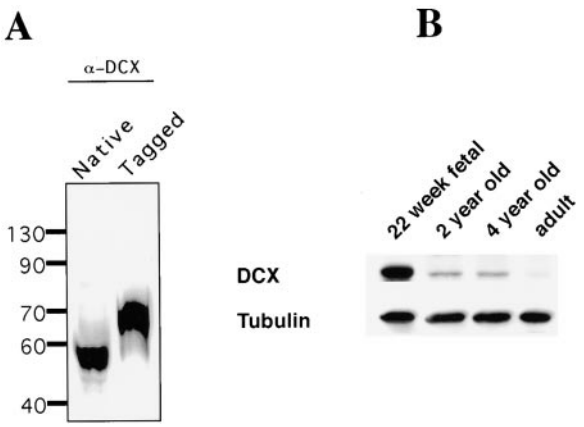

Figure 1. DCX Is Developmentally Regulated

(A) Immunoblot analysis demonstrating specificity of α-DCX antisera. Whole cell extract from cultured neurons or COS7 cells transfected with an epitope-tagged expression vector encoding DCX was probed with α-DCX. α-DCX produces a single specific band, both in cultured neurons (55 kDa) and as a HIS-tagged fusion protein in overexpressing COS7 cells (65 kDa).

(B) Developmental regulation of DCX in human occipital cortex of various ages. Blots were probed with α-DCX and subsequently probed with α-tubulin to control for protein loading. DCX is highly expressed during embryonic life and rapidly downregulated, with little detectable signal in the adult.

by affecting microtubule bundling. Additionally, overexpressed DCX strongly colocalizes with microtubules and leads to striking microtubule bundling that is resistant to depolymerization with colchicine. These results suggest that DCX may affect migration through its effects on microtubule organization or stabilization.

Results

DCX Is Expressed Exclusively in Postmitotic Neurons during Periods of Migration

To date, there is little information about the temporal and spatial pattern of DCX expression (des Portes et al., 1998; Matsuo et al., 1998). To address this, we generated polyclonal antisera to a peptide immunogen corresponding to the carboxyl terminus of the DCX protein. In order to test the specificity of α-DCX antisera, Western blots of cultured neurons and of COS7 cells transfected with epitope-tagged DCX were probed. On Western analysis, the α-DCX antisera recognized a single 55 kDa band in lysates of cultured neurons, and an appropriate single 65 kDa band in lysates of epitope-tagged DCX overexpressed in COS7 cells (Figure 1A), indicating that the antisera could be used to study the expression of DCX. The electrophoretic mobility of DCX is shifted by 15 kDa, because the predicted molecular weight of DCX is 40 kDa (des Portes et al., 1998; Gleeson et al., 1998). The electrophoretic mobility shift may be due to highly charged residues or to posttranslational modification. Recombinant DCX expressed in *E. coli* has a mobility of ~50 kDa, which suggests that DCX displays some electrophoretic mobility shift due to the primary amino acid sequence alone but does not exclude the possibility that DCX undergoes some posttranslational modification. This posttranslational modification may include phosphorylation, since DCX contains consensus sites for tyrosine phosphorylation by c-Abl and serine phosphorylation by microtubule-associated protein (MAP) kinases (Gleeson et al., 1998).

In order to understand the developmental regulation of DCX in humans, fresh occipital cortex from postmortem specimens at several ages were analyzed by Western blot. DCX was previously shown to be expressed predominantly in the brain, and at high levels only during development, based on Northern analysis of human tissues (Gleeson et al., 1998). Based on Western analysis, DCX was highly expressed at 22 weeks gestation and at lower levels during the early childhood developmental time points of 2 years and 4 years of age (Figure 1B). Very little DCX expression was detected in adult brain, consistent with the suggestion that DCX likely exerts its major effects during brain development.

DCX showed widespread but specific expression throughout the developing central and peripheral nervous system in mice, based upon immunoreactivity (Figure 2). DCX preimmune sera produced no appreciable signal in tissue sections (data not shown), indicating that the DCX signal observed with the postimmune sera is specific for DCX. DCX was expressed at high levels in the developing cerebral cortex, lateral ganglionic eminence, thalamus, midbrain, hindbrain, cerebellum, spinal cord, and retina (Figures 2A–2D; Figures 2A, 2B, and 2D are E14 mouse and Figure 2C is P8 mouse). Moreover, DCX was also expressed in all elements of the developing peripheral nervous system studied, including the trigeminal ganglia, the dorsal root ganglia, the sympathetic ganglia, and the enteric plexus (Figure 2D). Cells expressing DCX were not common in the proliferative regions of the neural axis, but were prominent in regions that contain postmitotic neurons such as the intermediate zone and cortical plate of the developing cerebral cortex.

DCX Is Expressed by Both Radially and Tangentially Migrating Populations of Neurons in the Cerebral Cortex

In order to more precisely define the cell types within the cerebral cortex that express DCX, we analyzed several embryonic time points in greater detail (Figures 3A–3G) using both in situ hybridization and immunofluorescence. At E14, expression of DCX mRNA and protein was equally intense in the intermediate zone, subplate, and cortical plate. Expression was excluded from the ventricular zone, but occasional cells were positive in the subventricular zone (SVZ) (Figures 3A and 3B, arrows).

At E17, the expression of DCX was high both in the intermediate zone/subplate region, containing neurons that are actively migrating, and in a thin layer of cells at the upper margin of the cortical plate, containing neurons that have just completed their migration. The majority of DCX protein in the intermediate zone/subplate region appears to derive from migrating neurons in these regions and not from distantly derived cortical afferent fibers, because the DCX in situ hybridization signal closely matched DCX protein expression (Figures 3C and 3D). We could not, however exclude the possibility that a fraction of the DCX signal in the intermediate zone/subplate region derived from distant sources. The cortical expression of DCX mRNA and protein was highest in a thin layer of cells at the upper margin of the

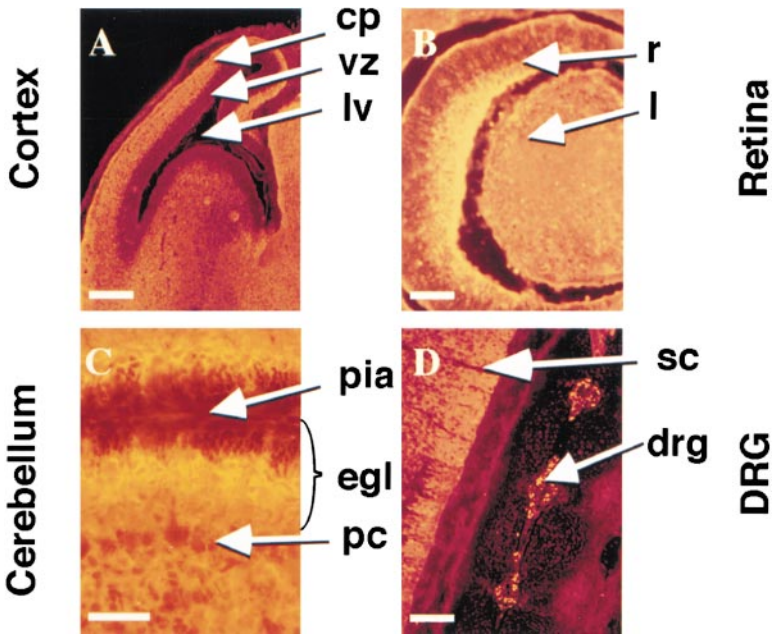

Figure 2. DCX Is Expressed by Migrating Neurons in the Central and Peripheral Nervous System

All tissues are from mouse at E14 in the sagittal plane except for the cerebellum, which is from P8, and are processed for DCX immunofluorescence. DCX is expressed by postmitotic cortical neurons (A), by retinal neurons in the ganglion cell layer (B), by granule cell neurons in the egl (C), and by spinal cord neurons as well as peripheral neurons in the drg (D). Abbreviations: cp, cortical plate; vz, ventricular zone; lv, lateral ventricle; r, retina; l, lens; egl, external granule layer; pc, Purkinje cell; sc, spinal cord; drg, dorsal root ganglion. Scale bars: 250 μm (A), 100 μm (B and C), and 200 μm (D).

cortical plate (arrow in Figure 3D), whereas neurons in the deeper cortical layers showed decreased levels of expression (box in 3D). To determine whether this layer of intense DCX expression localized to the marginal zone or to the newly arrived population of cortical plate neurons, we colabeled with anti-Reelin antibody, which specifically labels horizontally oriented Cajal-Retzius pioneer neurons in layer 1 (Ogawa et al., 1995). The intense DCX signal was visible in neurons just beneath the Reelin-positive Cajal-Retzius cells (Figure 3E), suggesting that neurons at the top of the cortical plate (which represent cells that are just finishing their radial migratory phase) express the highest levels of DCX, with this expression then rapidly downregulated. The deeper layers of the cortical plate (representing neurons that had finished their migration days previously) showed lower levels of expression of DCX, whereas neurons in the intermediate zone that were presumably still migrating also showed high levels of expression. The apparent downregulation of DCX in the cortical plate appears to be at least in part transcriptional, since DCX in situ hybridization also showed a decrease in mRNA expression in the deeper cortical plate layers (Figure 3C). At P0, the mRNA and protein expression of DCX in the cerebral cortex remained high but had become more diffuse with somewhat higher levels of expression in the SVZ (Figures 3F–3G). DCX expression in the cortex is then downregulated to undetectable levels by 2 weeks of age in the mouse.

DCX is highly expressed by neurons that appear to be migrating both radially and nonradially in the cortex. All newly postmitotic neurons, including those in the subplate region and in the cortical plate, appear to express high levels of DCX, suggesting that all migrating neurons in the cortex express DCX. Because of the high density of these neurons, individual neurons oriented radially in whole brain could not be well isolated. Therefore, in order to confirm that radially migrating neurons express DCX, individual radial migration units were isolated using the cortical imprint method and identified by phase microscopy (Anton et al., 1996). Using this method, glial fibers immunoreactive for the monoclonal Rat-401 antibody (Hockfield and McKay, 1985) were found to contain DCX-positive neurons along their shaft (Figures 2H–2K), providing direct evidence for DCX expression among populations of radially migrating cortical neurons. We next tested the possibility that nonradially migrating neurons also express DCX, by examining DCX immunoreactivity in the horizontally oriented TuJ1-positive neurons that O'Rourke et al. (1997) had identified as tangentially migrating based upon time-lapse imaging. At all stages, we observed a 1:1 correspondence in immunoreactivity of TuJ1 and DCX in horizontally oriented neurons in the SVZ (Figures 3L–3N), suggesting that tangentially migrating neurons also express DCX.

DCX expression in late postnatal and adult stages was identified in populations of neurons previously shown to be migrating to the olfactory bulb. Neuronal migration continues into adulthood in a well-defined population of neurons that proliferates in the SVZ, migrates along the rostral migratory stream (RMS), and is destined for the olfactory bulb (Lois and Alvarez-Buylla, 1994). We obtained sections in the adult mouse through the RMS in order to test the hypothesis that these neurons also express DCX. As expected, the RMS was found to consist of GFAP-immunoreactive glial "tubes" surrounding TuJ1-immunoreactive horizontally oriented neurons that had previously been shown to be migrating (Lois et al., 1996). We found that all of the TuJ1-immunoreactive cells in the RMS were also immunoreactive for DCX (Figures 3O–3Q) and that DCX-immunoreactive neurons were surrounded by GFAP-immunoreactive glial "tubes" (Figure 3R). This suggests a possible role for DCX in postnatal neuronal migration and suggests that DCX may be a general marker for newly postmitotic migrating neurons in many parts of the nervous system.

DCX Is Expressed by Both Cerebellar Purkinje and Granule Cells during Periods of Migration

DCX was also strongly expressed by neurons in the cerebellum during periods of migration. Since more than

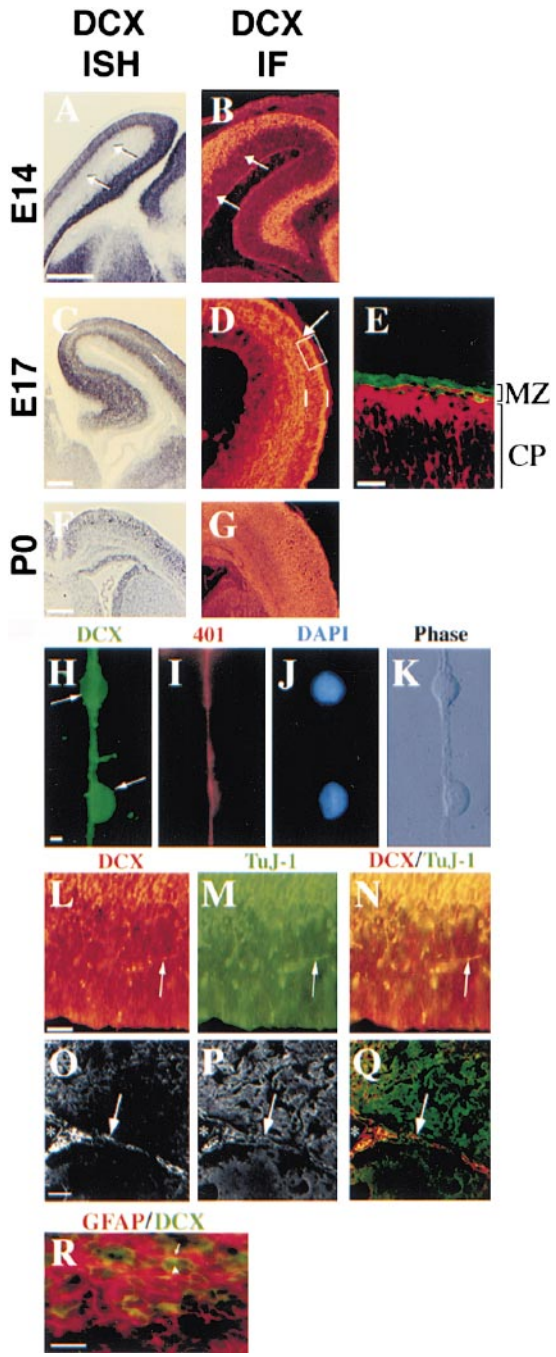

Figure 3. DCX Is Expressed by Migrating Neurons during Both Embryonic Development and Adulthood and by Populations of Both Radially and Nonradially Migrating Neurons

(A–G) DCX is expressed by postmitotic neurons in the developing cerebral cortex. DCX is first expressed by scattered cells in the subventricular and intermediate zones (arrows), as seen in the sagittal plane at E14 (A and B) by in situ hybridization (ISH) and immunofluorescence (IF). Expression continues at high levels at E17 as seen in the coronal plane (C and D) in the developing cortical wall, with the highest level of expression beneath the cortical plate and at the margin of the cortical plate (arrow in [D] indicates the top of the cortical plate, lines in [C] and [D] delineate the margins of the cortical plate), with lower levels of expression in neurons in the deeper cortical plate that completed migration earlier. (E) shows a higher-power view of boxed image in (D), immunolabeled for DCX (red) and Reelin (green). Reelin is expressed by Cajal-Retzius neurons in the marginal zone (MZ), and DCX is expressed in cortical plate neurons (CP). High levels of DCX immunoreactivity are detected in neurons at the uppermost part of the cortical plate, representing the most recently arrived neurons, adjacent to the Reelin-expressing cells. (F) and (G) show the DCX expression at P0 as seen in the coronal plane is more diffuse in the cortical wall, with some areas showing persistent low levels of expression. Scale bars: 250 μm (A–D), 50 μm (E), 500 μm (F and G).

(H–K) DCX is expressed by radially migrating neurons. Cortical migratory imprints of individual radial units, demonstrating two neurons (arrows in [H]) expressing DCX that are closely apposed to a radial glial fiber. The neurons are reactive for DCX (H), while the radial glial fiber is immunoreactive for Rat-401 antibody (I). DAPI staining demonstrates the nuclei of the two neurons (J), while phase microscopy demonstrates the morphology of the radial migratory unit (K). Scale bar: 10 μm.

(L–N) DCX is expressed by nonradially migrating neurons. Immunofluorescence of DCX (L) and TuJ1 (M) and colabeling (N) from the SVZ region of mouse E14 intermediate zone. Neurons with a horizontal morphology that label with α-DCX also label with α-TuJ1 (arrows in [L] through [N]), suggesting that they belong to the population of tangentially migrating neurons (O'Rourke et al., 1997). Scale bars: 10 μm (H and I), 250 μm (K–M).

(O–R) DCX is expressed by populations of neurons migrating to the olfactory bulb in the adult. Sagittal section through the SVZ of an adult mouse (>P30). Neurons expressing DCX (O) are also immunoreactive for TuJ1 (P), as evidenced by the merged image (Q). The arrow highlights the rostral migratory stream, and the asterisk indicates the lateral ventricle. (R) shows a sagittal section through the rostral migratory stream of an adult mouse (>P30). GFAP-immunoreactive glial "tubes" (red, arrow) contain DCX-immunoreactive neurons (green, arrowhead). Scale bars: 100 μm (N–P), 50 μm (R).

one cell type in the cerebellum expresses DCX, individual populations of neurons were identified by colabeling with identifying markers. Calbindin-immunoreactive Purkinje cells (Nordquist et al., 1988) expressed high levels of DCX during periods of migration (Figures 4B–4D). Whereas calbindin immunoreactivity is diffusely positive in the cellular cytoplasm, DCX immunoreactivity appeared to be predominantly localized to the periphery of the soma under confocal microscopy, suggesting that DCX may have a specific subcellular localization in migrating neurons. Z series reconstruction of confocal images (data not shown) confirmed that the source of DCX immunoreactivity was indeed Purkinje cells and not neighboring cells.

We also confirmed that granule cells express high levels of DCX during the period of radial descent into the cerebellum. There was a lack of expression of DCX in the "premigratory" mitotically active granule cell precursors in the external granule layer (EGL), but there were high levels of expression in the deeper populations of granule cells that have been previously shown to migrate radially along Bergmann glia fibers (Hatten and Heintz, 1995). In order to be certain that the source of DCX immunoreactivity was indeed from granule cells, cerebellar sections were colabeled with TAG-1, which specifically labels granule cells at an early stage of radial descent (Stottmann and Rivas, 1998). As expected, the DCX-expressing granule cells were found to colabel with TAG-1 in populations of granule cells both superficial to and deep to the Purkinje cell layer (Figures 4E–4G). TAG-1 is a glycosyl-phosphatidylinositol-linked (GPI-linked) membrane-bound protein (Furley et al., 1990), allowing subcellular localization of DCX relative to the

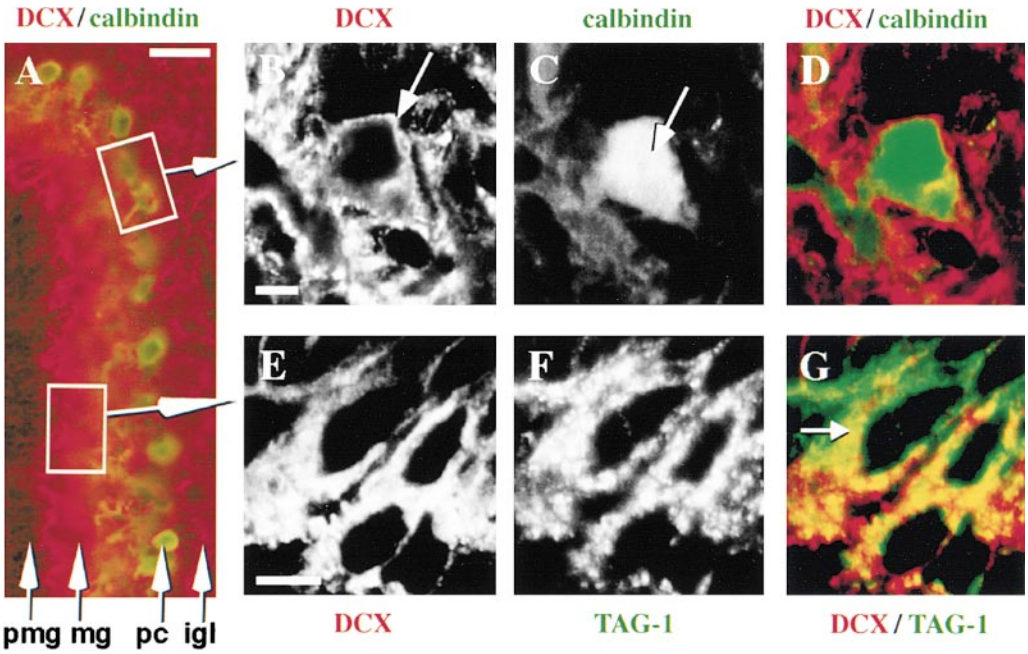

Figure 4. DCX Is Expressed by Populations of Migrating Purkinje and Granule Cells

(A) Immunofluorescence using α-DCX (red) and μ-calbindin (green) antibodies from mouse cerebellum at P8, in order to orient the figures below. Abbreviations: pmg, premigratory granule cells; mg, migratory granule cells; pc, Purkinje cells; igl, internal granule layer. Boxes indicate areas of higher power confocal images in (B) through (D) and (E) though (G). Scale bar: 70 μm.

(B–D) DCX is expressed in populations of migrating Purkinje cells. Confocal microscopy of P0 cerebellum showing immunoreactivity to DCX (arrow in [B]) and calbindin (arrow in [C]) in a single Purkinje cell. DCX and calbindin do not colocalize, but instead DCX immunoreactivity appeared to be predominantly localized to the periphery of the soma. Scale bar: 10 μm.

(E–G) DCX is expressed in populations of cerebellar granule cells during periods of radial migration. Confocal microscopy of P8 cerebellum showing immunoreactivity of DCX (E) and TAG-1 ([F], to identify postmitotic radially migrating granule cells), to demonstrate that the two proteins are expressed in the same population of cells (arrow in [G]). Scale bar: 10 μm.

region of the plasma membrane with confocal microscopy. Similar to what was observed for DCX immunoreactivity in migrating Purkinje cells, DCX immunoreactivity appeared to be predominantly localized to the periphery of the soma, further suggesting that DCX may have a specific subcellular localization in migrating neurons.

DCX Localization Overlaps with Microtubules in Cultured Neurons, and This Localization Is Disrupted by Colchicine

In order to more carefully analyze the subcellular localization of DCX, we analyzed DCX localization in cultures of primary cortical neurons. DCX was present predominantly in the periphery of the soma of cultured neurons in a ring-like distribution around the nucleus, similar to what was observed in cerebellar sections. DCX immunoreactivity was clearly fibrillar in cultured neurons under high-power microscopy (Figures 5B and 5F, arrows), suggesting it may be associated with one or more cytoskeletal elements. We therefore examined three common cytoskeletal constituents for colocalization with DCX. When cultured neurons were colabeled with DCX and markers for actin, neurofilaments, and microtubules, a closely overlapping distribution was observed only for DCX and microtubules (Figures 5A–5D). DCX and microtubules produced similar patterns of immunoreactivity in the soma of cultured neurons, giving the appearance of strands surrounding the nucleus. The DCX immunoreactivity was somewhat punctate and more diffuse than microtubule immunoreactivity, but MAPs such as MAP2 and tau also produce a somewhat punctate and diffuse immunoreactive pattern in neurons (Matus et al., 1986; Tint et al., 1998). The overlapping pattern of DCX and microtubule immunoreactivity was most notable surrounding the nucleus and extending into the proximal neurites; there was less DCX immunoreactivity in proximal neurites and very little immunoreactivity in distal neurites and growth cones, whereas tubulin immunoreactivity extended the full length of the neurites (data not shown). Localization of DCX and microtubules was further investigated by colabeling with DCX and other microtubule antibodies, including TuJ1, tyrosinated tubulin, and acetylated tubulin antibodies as well as colabeling with a MAP2 antibody (pan MAP2). DCX immunoreactivity closely overlapped with each of these microtubules or MAPs (TuJ1 is shown in Figures 5E–5H), providing further evidence for a possible association of some DCX with the microtubule cytoskeleton. DCX showed no evidence of colocalization with either actin fibers or neurofilaments (data not shown), suggesting that the fibrillar expression pattern of DCX is specific to microtubules.

Whereas disruption of microtubules disrupts the fibrillar DCX staining, disruption of actin enhanced the colocalization of DCX with microtubules. Primary cortical

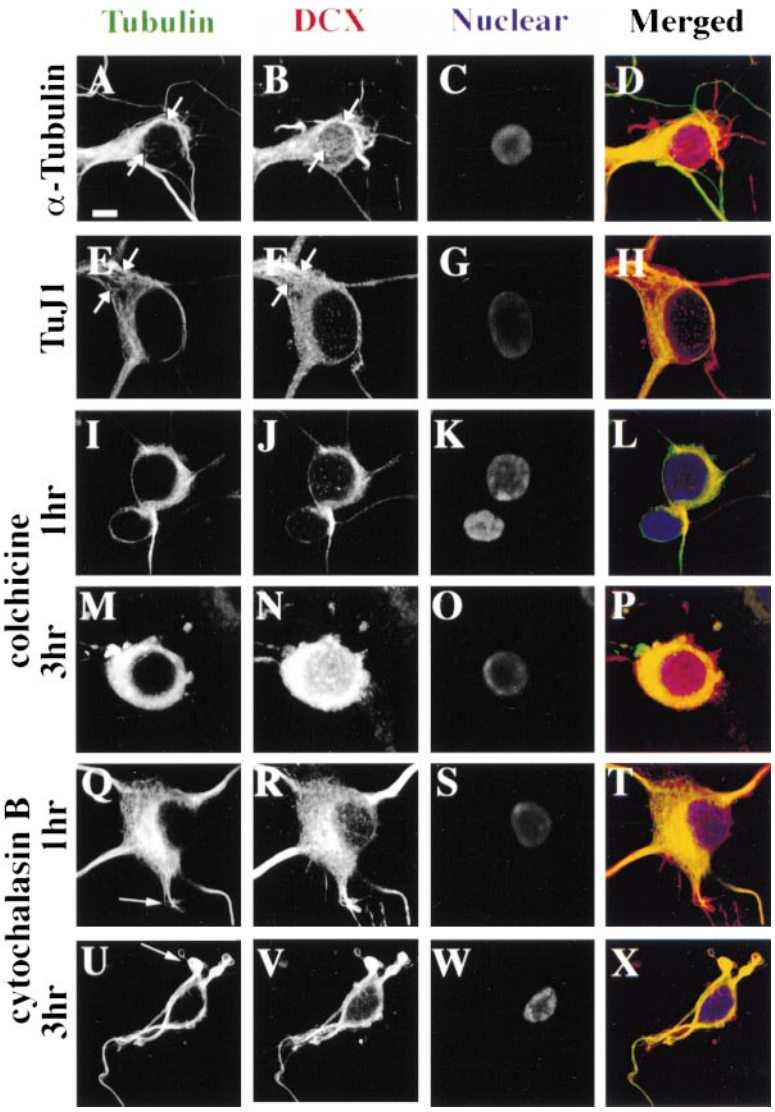

Figure 5. DCX Localization Overlaps with Microtubules in Primary Cortical Neurons, and DCX Localization Is Disrupted by Colchicine but Not by Cytochalasin B

(A–H) DCX immunoreactivity from untreated E17 rat primary cortical neurons to demonstrate overlapping expression of DCX with microtubules using two different anti-microtubule antibodies (against α-tubulin and TuJ1). DCX shows overlapping immunolocalization with tubulin in individual microtubule fibers and in microtubules bundles (arrows). (I–X) The overlapping localization of DCX with microtubules is disrupted by colchicine but not by cytochalasin B. Primary cortical neurons were treated with either colchicine or cytochalasin B for 1 or 3 hr and processed for microtubule and DCX immunoreactivity. At 1 hr, there is some loss of the microtubule cytoskeleton, and DCX no longer colocalizes with the remaining microtubule cytoskeleton. At 3 hr, the microtubule cytoskeleton is completely disrupted, and DCX immunoreactivity is no longer fibrillar. Treatment with cytochalasin B for 1 or 3 hr disrupted the actin cytoskeleton, with resultant process retraction into curled structures (arrows in [Q] and [U]), but left the microtubule cytoskeleton intact. DCX retains its overlapping expression with microtubules after cytochalasin B. Nuclear stain is TOTO-3. Scale bar: 10 μm.

neurons that were maintained for two days in culture were exposed to 10 μg/ml colchicine or vehicle control for 1–3 hr and immediately fixed. This treatment led to a slow disruption of the microtubule cytoskeleton but did not significantly affect the actin cytoskeleton (data not shown), with retention of some neurites over the course of the experiment. Over the 3 hr time course, the microtubule cytoskeleton collapsed, leading to a distinct change in the subcellular distribution of tubulin. The distribution of DCX over the 3 hr time period was similarly but more severely affected, with a nearly complete change in the distribution of DCX from a fibrillar pattern in the periphery of the soma to a diffuse distribution within the soma, with some possible DCX immunoreactivity within the cell nucleus (Figures 5I–5P). In contrast, disruption of actin filaments with 5 μg/ml cytochalasin B (Figures 5Q–5X) did not disrupt the fibrillar staining pattern of DCX and in fact tended to enhance the colocalization of DCX with microtubules. This data suggests that the filamentous perikaryal localization of DCX is dependent on an intact microtubule cytoskeleton.

DCX Coassembles with Microtubules from Brain

To test whether the overlapping DCX localization with microtubules in cultured neurons indicates a physical interaction, microtubules were assembled from the cytosolic fraction of brain and examined for the presence of DCX. In this experiment, half of the cytosolic fraction was treated with taxol and half was untreated. DCX was intensely enriched in the taxol-stabilized microtubule pellet, with approximately two-thirds of DCX protein coassembling with microtubules (Figure 6A). When taxol was excluded from the sample, tubulin polymerization was minimal and DCX was not detected in the pellet. As controls, the same Western blot from this experiment was reprobed with antibodies to a known MAP (MAP2C) and a protein that is not known to associate with microtubules (mDab1). As expected, MAP2C was present nearly exclusively in the microtubule fraction, whereas mDab1 did not coassemble with polymerized microtubules (Figure 6A). We also reprobed this Western blot for the presence of LIS1. Approximately 25% of LIS1 was detectable in the microtubule pellet, with the majority

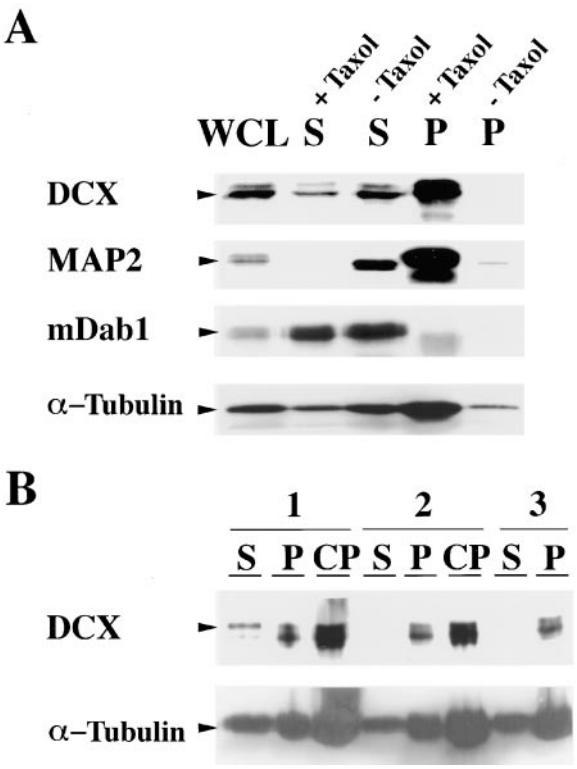

Figure 6. DCX Coassembles and Cycles with Microtubules

(A) DCX coassembles with taxol-stabilized microtubules from rat brain. Whole brain lysate from P5 newborn rat pups were cleared by centrifugation in order to isolate a tubulin-rich fraction and divided into two equal aliquots. To one aliquot, taxol and GTP were added, and to the other aliquot, GTP alone was added and microtubules were isolated by centrifugation. DCX is enriched in the taxol-stabilized microtubule pellet, with smaller amounts remaining in the supernatant. Reprobing the same blot with α-pan MAP2 shows that the DCX enrichment is similar to MAP2C. In contrast, mDab1 does not coassemble with microtubules. The tubulin content of each sample is also indicated (α-tubulin). Abbreviations: WCL, whole cell lysate; S, supernatant; P, microtubule pellet.

(B) DCX continues to coassemble with microtubules over several depolymerization/repolymerization cycles, but a significant fraction associates with cold-stable microtubules. Cell lysate from COS cells overexpressing DCX was added to a crude microtubule preparation, depolymerized, repolymerized, and centrifuged, and aliquots were taken from the supernatant (1S) and the pellet (1P). The sample was cold depolymerized and recentrifuged in order to remove the cold-stable microtubule fraction (1CP), and the remaining supernatant was cycled twice more (2S, 2P, and 2CP refer to the second cycle; 3S and 3P refer to the third cycle). After the first cycle, DCX was found in both the pellet and the cold pellet and was no longer found in the supernatant. The tubulin content of each sample is also indicated (α-tubulin).

remaining in the supernatant (data not shown), which is consistent with a previous report (Sapir et al., 1997). The proportion of DCX that coassembles with microtubules is considerably greater than for LIS1, suggesting that the association of DCX with microtubules may be more direct or more stable than that for LIS1. Similar results for DCX were obtained after three cycles of polymerization and depolymerization of tubulin, with little DCX remaining in the supernatant (Figure 6B). Interestingly, a significant fraction of DCX continued to associate with the cold-stable microtubule fraction after each cycle, suggesting that DCX may be associated with cold-stable microtubule formation. Together, these data suggest that DCX physically interacts with the microtubule cytoskeleton, either through a direct interaction with microtubules or indirectly through a bridging protein partner.

DCX Stimulates Microtubule Polymerization

Based on the coassembly of DCX with brain microtubules, we hypothesized that DCX binds directly to tubulin to affect microtubule polymerization or stability. This hypothesis was tested using a turbidimetric assay to test the ability of recombinant DCX to affect the polymerization rate of phosphocellulose-purified (>99% pure) tubulin. In this assay, monomeric tubulin causes minimal diffractive interference to transmitted light as measured by the detection of light at a 90° angle to the transmitted beam in a real-time fluorimeter. As tubulin polymerizes, the turbidity of the solution increases, which is measured by an increase in diffracted light (Gaskin et al., 1974). The tubulin concentration in this experiment was just below the critical concentration for spontaneous polymerization, so little polymerization occurred in the absence of microtubule effectors. Recombinant DCX was added to the reaction at increasing concentrations, and a concentration-dependent increase in turbidity resulted. At all concentrations tested, DCX had a measurable effect on the turbidity in this assay (Figure 7A). Both the rate and the total extent of turbidity were enhanced in the presence of DCX. Recombinant MAP2C had a similar but somewhat more pronounced effect than that observed for DCX. Negative stain electron microscopic analysis of the DCX-polymerized tubulin demonstrated extensive arrays of polymerized microtubules and microtubule bundles (Figures 7B and 7C), indicating that the increase in turbidity reflected genuine microtubule polymerization. Coomassie analysis of the pellets and the supernatants from this experiment demonstrated that DCX was highly enriched in the polymerized microtubule pellet with ~1:10 stoichiometry of DCX to monomeric tubulin (data not shown), suggesting that DCX directly binds to microtubules in this assay. These data support a role for DCX in binding directly either to tubulin dimers or to microtubules to enhance polymerization.

The DCX effect on microtubule polymerization is likely through bundling of microtubules, without a measurable effect on the overall length of microtubules. This was determined by examining the effect of recombinant DCX on rhodamine-labeled phosphocellulose-purified tubulin. DCX was added to tubulin over the concentration range of 0.01–0.7 mg/ml, while maintaining tubulin at the critical concentration of 0.5 mg/ml. In the presence of DCX at concentrations above 0.02 mg/ml, fluorescent tubulin formed dramatic aster-like "stars," with from two to ten bundled microtubule fibers emanating from the center (Figures 7D and 7E). The center of the star likely represents DCX associated with tubulin, since neither tubulin nor DCX forms these stars in the absence of the other. The mean length of the microtubule fibers was not significantly different in the absence or presence of DCX (13 versus 11 arbitrary units; Figure 7F), but there

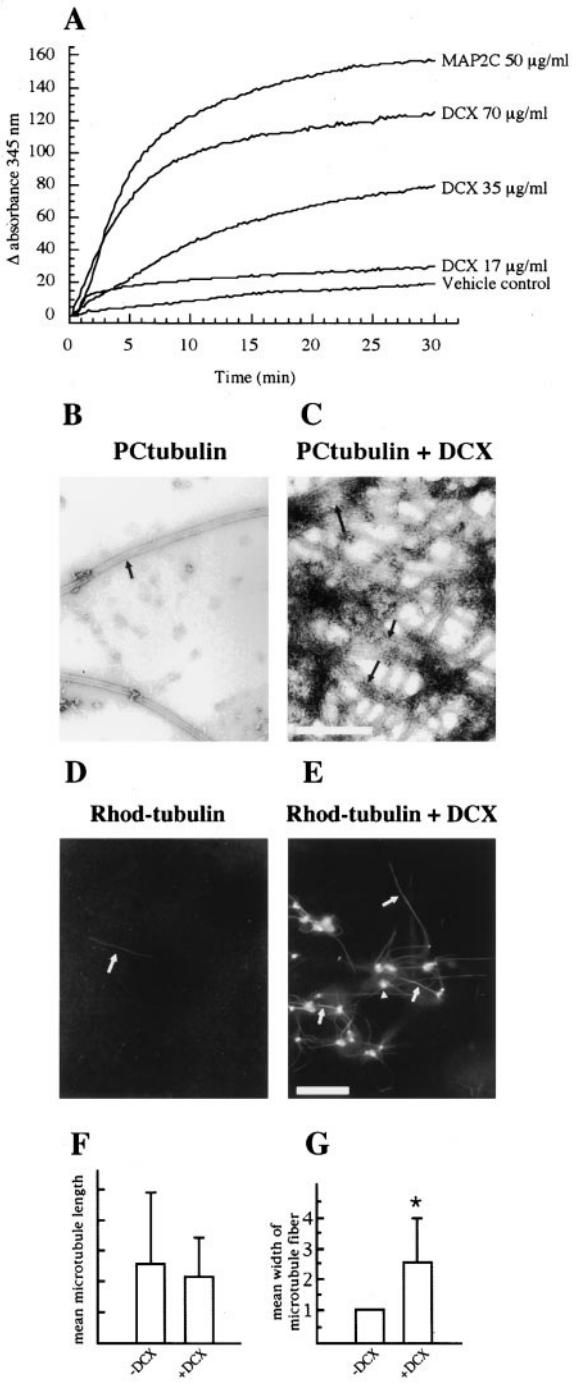

Figure 7. DCX Leads Directly to Microtubule Polymerization, Possibly through an Effect on Microtubule Bundling

(A) Recombinant DCX directly affects tubulin polymerization. Vehicle, recombinant MAP2C, or recombinant DCX at various concentrations was added to 10 mg/ml phosphocellulose-purified tubulin (>99% pure) in the presence of 1 mM GTP, and the degree of polymerization, as measured by turbidity, was recorded over 30 min. At time zero, the reading was standardized to zero diffraction (Δ absorbance 345). DCX had an effect comparable to recombinant MAP2C, with an increase in the rate and total amount of tubulin polymerized to microtubules, but the effect was somewhat smaller in magnitude.

(B–G) Recombinant DCX leads to an increase in microtubule bundling, with no net effect on microtubule length.

were many more microtubules in the presence of DCX, as quantitated by the turbidity assay. Microtubules were also significantly brighter in the presence of DCX, suggesting that microtubules were present in bundles. In order to assay for a potential effect of DCX on microtubule bundling, tubulin polymerized in the presence and absence of DCX was examined by negative stain electron microscopy to identify individual microtubule fibers. Self-assembled microtubules in the absence of DCX were always monomeric, whereas microtubules assembled in the presence of DCX were often bundled. This difference was quantitated by counting the number of individual microtubules that self-associate in the presence and absence of DCX. There is a statistically significant difference in the bundling of microtubules in the presence of DCX (average of 2.51 microtubules bundled in the presence of DCX versus no bundling without DCX, respectively, $p < 0.001$; Figure 7G), further suggesting that DCX has a significant effect on bundling of individual microtubules in this assay. The possibility that DCX may nucleate microtubules was not specifically addressed by this experiment, although it remains a possibility. Taken together, these data suggest that recombinant DCX leads directly to polymerization of tubulin in vitro, apparently by bundling microtubules.

Overexpression of DCX Leads to a Striking Microtubule Phenotype

Based upon the previous experiments, we hypothesized that the overexpression of DCX in cells may be associated with an effect on microtubules or cellular morphology. We therefore overexpressed epitope-tagged DCX in cortical cultures and examined for an effect on microtubules. Tight colocalization of DCX with the microtubule cytoskeleton was observed when visualized with the epitope antibody, whereas cells overexpressing a negative control tagged lacZ gene, using the same epitope antibody, showed diffuse immunoreactivity (Figures 8A–8F). This was most apparent in transfected

(B and C) Negative stain electron microscopy (25,000×) of phosphocellulose-purified tubulin (PC tubulin) (1 mg/ml) in the absence of DCX (B) and in the presence of 35 μg/ml DCX (C). In the absence of DCX, microtubules were present as single tubules (arrow). When DCX was added, microtubules were much more numerous and appeared to emanate from electron-dense centers in three or four microtubule bundles, each consisting of several (two to eight) individual microtubules (arrows). Scale bar: 250 nm.

(D and E) Fluorescence image of rhodamine tubulin plus PC tubulin (0.5 mg/ml) in the absence of DCX (D) and in the presence of 0.01 mg/ml recombinant DCX (E). In the absence of DCX (D), single microtubules were notable (arrow). The addition of DCX (E) led to a significant increase in the number of microtubules, as well as the formation of aster-like "stars" (arrowhead). Microtubules emanating from these aster-like "stars" appeared to be bundled (arrow in [E]), as evidenced by the increased intensity compared to untreated microtubules in (D). Scale bar: 250 μm.

(F and G) Quantitation of mean microtubule length and mean width of microtubule fibers in the absence and presence of DCX. In (F), no significant difference in mean microtubule length was noted with the addition of DCX under fluorescence microscopy. In (G), in the absence of DCX, microtubules were never found to be bundled but were often bundled in the presence of DCX (asterisk indicates $p < 0.001$) based upon electron microscopic analysis.

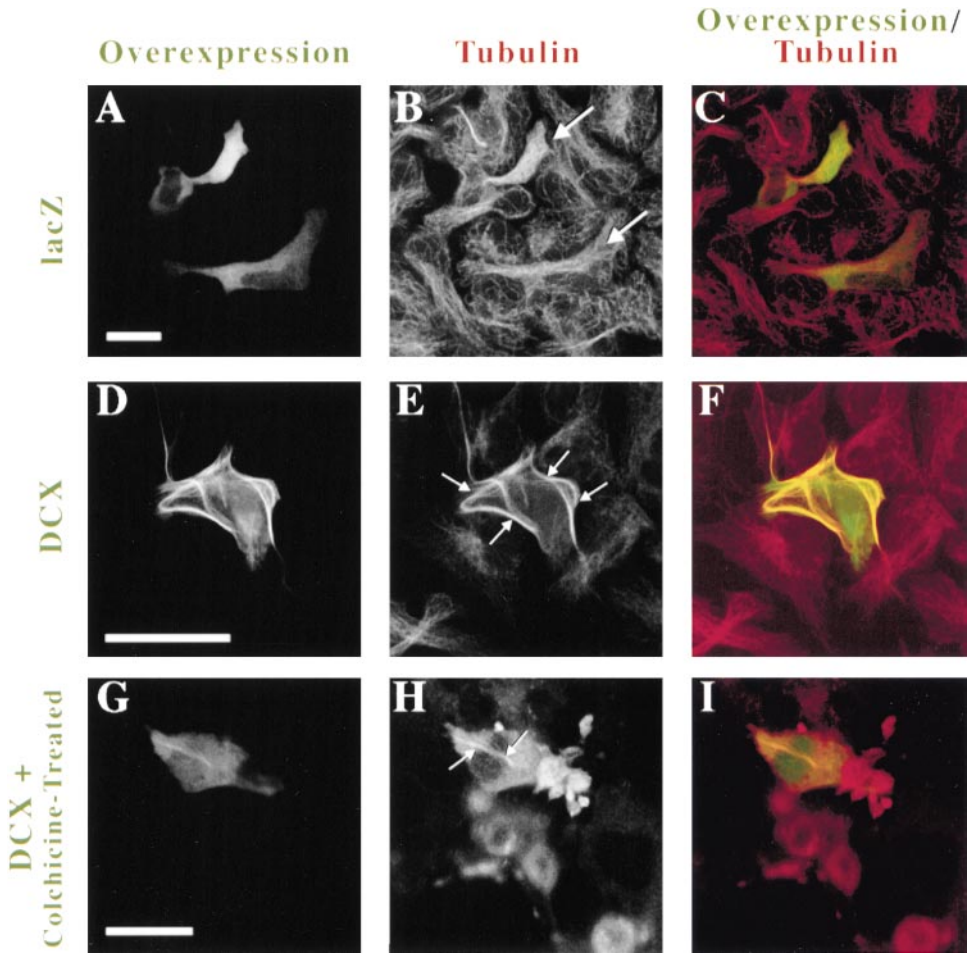

Figure 8. Overexpression of DCX in Cultured Neural Cells Leads to a Striking Microtubule Phenotype, and These Microtubules Are Resistant to Depolymerization with Colchicine

(A–C) LacZ overexpression in neural cells (likely glia) from a primary cortical culture was distributed diffusely within the cytoplasm (arrows in [B]).

(D–F) Overexpressed DCX colocalizes with the microtubule cytoskeleton and leads to the induction of microtubule bundles in the periphery of the cell soma (arrows in [E]).

(G–I) Microtubule bundles induced by the overexpression of DCX (arrows in [H]) are resistant to colchicine treatment, whereas microtubules in neighboring cells are completely disrupted by colchicine. Scale bar: 50 μm.

nonneuronal cells, which represent astrocytes and oligodendrocytes, likely because these cells have a flattened morphology and thus the cytoskeleton is more easily appreciated. In ~50%–75% of these neural cells expressing the DCX epitope tag, we observed a striking alteration in the microtubule cytoskeleton compared to a lacZ negative control. The microtubule cytoskeleton in these flat neural cells was largely bundled and had the appearance of whorls at the periphery of the cell soma, or multiple long bundles of microtubules, which appeared to distort the morphology of the cell. The microtubule cytoskeleton of *neurons* overexpressing DCX did not appear to be significantly different from untransfected neurons (data not shown), possibly due to endogenous levels of DCX in neurons or differential regulation of binding partners in neurons versus glia. In transfected neurons, epitope-tagged DCX tightly colocalized with the microtubule cytoskeleton, confirming the overlapping expression pattern observed for native DCX with microtubules. These results together suggested that overexpression of DCX in neural cells that do not normally express DCX leads to a direct change in the microtubule cytoskeleton.

We considered whether the bundles of microtubules observed in DCX-overexpressing cells would be resistant to the depolymerizing effects of colchicine, as is the case when other MAPs are overexpressed (Takemura et al., 1992). We therefore transfected primary cortical cultures with epitope-tagged DCX or negative control epitope-tagged lacZ and, after 2 days, induced microtubule depolymerization with colchicine treatment for 2 hr. The cells were subsequently fixed and processed to visualize DCX or lacZ with the tagged antibody, as well as microtubules. Although the DCX fibrillar immunoreactivity is much less pronounced after microtubule depolymerization, we found a significant effect of DCX on the colchicine stability of microtubule bundles in all transfected cells (Figures 8G–8I) compared to either

lacZ-transfected cells (data not shown) or neighboring untransfected cells. This suggests that DCX leads to the formation of stable microtubule bundles when overexpressed and supports the in vitro association of DCX in cold-stable microtubules and in microtubule bundle formation.

Discussion

Here, we show that DCX is expressed by newly postmitotic, migrating neurons both in the central and peripheral nervous system, suggesting that it may potentially play a role in neuronal migration throughout the nervous system. DCX is expressed by neurons that appear to be migrating both radially and nonradially. The neuronal expression of DCX in cultured neurons suggests a distinct localization to the periphery of the cell soma, in a pattern overlapping with microtubules, and this colocalization is disrupted by colchicine but not by cytochalasin B. DCX coassembles with microtubules from brain, and recombinant DCX leads to enhanced tubulin polymerization, apparently through an effect on microtubule bundling. Overexpression of DCX leads to striking alterations in the microtubule cytoskeleton, with the formation of distinct microtubule bundles that are resistant to the depolymerizing effects of colchicine. These results suggest that at least one of the roles of DCX in neuronal migration is likely through altering microtubule organization and stabilization. Our observations, together with the finding that LIS1 has effects on microtubules (Sapir et al., 1997), suggests that microtubule regulation is a key component of neuronal migration in the cerebral cortex.

DCX Expression Suggests a Cell-Autonomous Role in Neuronal Migration throughout the Nervous System

DCX is expressed in all populations of postmitotic migrating neurons, suggesting that it is at least a marker for these young neurons and may be playing a role in neuronal migration throughout the developing nervous system. We observed high levels of expression of DCX in cortical neurons that appear to be migrating radially as expected, but it was also present at high levels in cortical neurons that appear to be migrating nonradially in the SVZ and in migrating cerebellar neurons. Strikingly, DCX was also expressed in the adult at high levels in newly postmitotic neurons from the SVZ that continue to proliferate and populate the olfactory bulb. The high levels of expression in the rostral migratory stream may provide at least a partial explanation for the reported high levels of expression of DCX in the frontal lobe, based on Northern analysis (Sossey-Alaoui et al., 1998). Certainly, in mice older than P5, we did not detect significant DCX expression by established neurons in the cortical plate, based upon in situ hybridization and immunohistochemistry. The widespread obligate expression in newly postmitotic migrating neurons throughout the nervous system suggests that DCX may play an essential role in these migrations.

High levels of expression of DCX in neurons that appear to be migrating is consistent with the proposed cell-autonomous defect in neuronal migration in the mosaic double cortex phenotype. The widespread expression of DCX outside of the cerebral cortex is somewhat surprising, because the extracortical phenotype is not striking in patients with *DCX* mutations. In the only male patient with a *DCX* mutation who has been studied pathologically, the extracortical phenotype was mild (Berg et al., 1998) but included diffuse cerebellar atrophy and a decreased density of granule and Purkinje cells, with Purkinje cell heterotopias. The cerebellar dentate nucleus and inferior olive were simplified with decreased neuronal density. These developmental abnormalities are consistent with the strong expression pattern of DCX in migrating cerebellar Purkinje and granule cells and with the expression in the brainstem. However, no phenotype was reported in other neuronal tissues that we found strongly express DCX, including the spinal cord, retina, and peripheral ganglia. Our findings of more widespread DCX expression outside of the cerebral cortex should stimulate a search for additional extracortical defects among patients with *DCX* mutations.

The striking change in DCX expression in neurons after migration into the cortex suggests that perhaps one or more extracellular signals present in the marginal zone or cortical plate may regulate the expression of DCX. DCX expression in neurons apposed to Cajal-Retzius neurons is very high, whereas neurons in the deeper layers of the cortical plate, which have just finished migrating in the preceding 1–2 days, show significantly decreased DCX expression levels. If an extracellular or secreted molecule in the vicinity of Cajal-Retzius cells does regulate DCX expression, then Reelin would be an excellent candidate, as Reelin has been shown to downregulate the protein level of mDab1 in neurons during their periods of migration (Rice et al., 1998). However, *reeler* mice do not demonstrate significantly altered levels of DCX expression, and the application of Reelin to primary cortical neurons does not alter the level of DCX expression (J. G. G., P. T. L., E. Olson, and C. A. W., unpublished data). Perhaps there are other extracellular signals that mediate the termination of migration, possibly by altering the expression levels of key neuronal migration genes.

Microtubules and Neuronal Migration

Our finding that DCX is a MAP is consistent with studies of migrating neurons suggesting that the microtubule cytoskeleton is essential, both in movement of the leading process and of the nucleus in the cell soma. In migrating cerebellar granule neurons, dynamic microtubules have been identified both in the leading process and in a "cage-like" distribution encircling the nucleus (Rivas and Hatten, 1995). In these cells, microtubules appear to form a bridge between the cell membrane and the soma, suggesting a role for microtubules and associated proteins in force generation, junction morphogenesis, and control of cell shape (Gregory et al., 1988). The distinct polarity of microtubules during neuronal migration, with the plus ends of the microtubules in the leading process uniformly facing the growing tip and the minus ends facing the nucleus, suggests that they may exert push and pull forces that contribute to the piston-like saltatory displacement of the nucleus and cytoplasm (Rakic et al., 1996). The expression of DCX

in the soma of neurons resembles the "cage" of tubulin surrounding the nucleus (Rivas and Hatten, 1995), suggesting that DCX may be involved in the regulation of this population of microtubules.

DCX May Define a New Family of Microtubule-Associated Proteins

The definition of a MAP is somewhat variable (Matus, 1988), although a strict definition of a MAP is a protein that binds to, stabilizes and promotes the assembly of microtubules (Desai and Mitchison, 1997). We demonstrate that DCX is a MAP, by showing that it colocalizes and coassembles with microtubules; it has a direct effect on microtubule polymerization, which is at least partially due to an effect on bundling; and, when overexpressed in cultured neural cells, it leads to a striking microtubule phenotypic change that is resistant to colchicine depolymerization. Although we did not evaluate for the possibility of a nonspecific toxic effect of colchicine on these DCX-transfected cells, the overall effects of DCX overexpression are strikingly similar to the effects of MAP2C or tau overexpression (Knops et al., 1991; Kaech et al., 1996), both of which also lead to distinct bundling patterns of microtubules that are resistant to depolymerization.

DCX may be one of the unidentified factors in neurons that endow cold stability to neuronal microtubules (Webb and Wilson, 1980; Black et al., 1984), since a significant fraction of microtubules in the presence of DCX remains resistant to cold depolymerization. To date, only the STOP (stable tubule only polypeptide) proteins have been implicated in this cold stability (Margolis et al., 1986; Denarier et al., 1998; Guillaud et al., 1998), but our data suggest that DCX may also be one of the proteins that leads to the unique microtubule properties of neurons, especially young neurons (Mareck et al., 1980) that express high levels of DCX.

Although the primary amino acid sequence of DCX lacks recognizable motifs, the clustering of disease-causing amino acid substitution mutations in two regions of the protein appears to define two critical domains (Gleeson et al., 1999). It will be interesting to see if one of these regions is responsible for binding to tubulin and regulating polymerization. DCX does not share amino acid homology with other MAPs, so the physical interaction between DCX and tubulin may define a novel tubulin binding domain. DCX shares 75% amino acid homology with a predicted protein KIAA0369 (GenBank accession number AB002367) (Gleeson et al., 1998), although KIAA0369 extends an additional 368 amino acids in the carboxy direction and appears to encode for a CaM kinase. Additionally, there are several other proteins that share significant amino acid homology with DCX in the database, suggesting that the DCX domain of these proteins may define a novel class of MAPs.

DCX, LIS1, and Nuclear Migration

The strikingly similar neuronal migration phenotype of lissencephaly in humans with *LIS1* mutations and those with *DCX* mutations suggested that perhaps the two proteins may function in concert in neuronal migration. LIS1 was shown to colocalize and coassemble with microtubules and to reduce microtubule catastrophe events (Sapir et al., 1997), suggesting that microtubule regulation may be one mechanism of action of LIS1. However, LIS1 was found to serve as a regulatory subunit of the enzyme platelet activating factor (PAF) acetylhydrolase (Hattori et al., 1994), an intracellular enzyme that hydrolyzes PAF, and as a homolog of NUDF in *Aspergillus* (Xiang et al., 1995; Morris et al., 1998), part of the genetic pathway regulating nuclear migration. LIS1 was also shown to copurify with p72syk, a splenic tyrosine kinase (Brunati et al., 1996), so that the actual mechanism by which LIS1 exerts its effect on neuronal migration has remained unclear. Our findings of a potential role for DCX in microtubule dynamics suggest that the most relevant of the proposed LIS1 interactions is with microtubules, and that microtubules likely play an important role in neuronal migration in the cerebral cortex.

The microtubule-related dependence on LIS1 for neuronal migration may be through nucleokinesis, based upon analysis of a LIS1 ortholog in *Aspergillus*, as well as a LIS1 binding partner found by yeast two-hybrid analysis. LIS1 displays 42% amino acid homology to the NUDF protein of the filamentous fungus *Aspergillus nidulans*. *nudf* was identified in a screen for mutants with defective nuclear translocation along the fungal mycelium (Xiang et al., 1995). NUDF displays more homology to LIS1 than to any other protein in the database, raising the possibility that LIS1 and NUDF are orthologs and that LIS1 may also function to translocate the nucleus. Additionally, a two-hybrid screen for LIS1-interacting proteins from a human library identified a homolog of NUDC that was expressed highly in brain (Morris et al., 1998), providing further evidence that the NUD pathway may be recapitulated in mammals. NUDF is a likely effector of NUDC, as NUDC affects the intracellular level of the NUDF protein, and overexpression of NUDF into the *nudC3* mutation strain restores nuclear migration (Xiang et al., 1995). While *nudC* encodes a novel protein, another *nud* gene, *nudA*, encodes the heavy chain of cytoplasmic dynein, a microtubule motor, and identifies cytoplasmic dynein as likely the main motor that catalyzes long-range nuclear migration in *Aspergillus* mycelium (Xiang et al., 1994). Taken together with biochemical evidence of LIS1 involvement in microtubule dynamics, this strongly suggests that LIS1 may exert its effect on neuronal migration by directing nucleokinesis. Our findings, which suggest a direct effect of DCX on microtubule dynamics, provide further compelling evidence for the involvement of microtubule dynamics in neuronal migration and suggest that LIS1 and DCX may function together through regulation of microtubules to direct nucleokinesis in migrating neurons.

Neuronal Migration Mutants May Define Three Distinct Phases of Cortical Neuronal Migration

Genetic analysis of mammalian neuronal migration suggests that it consists of three phases that can increasingly be viewed as separable. Mutations in *reelin* (D'Arcangelo et al., 1995), *mdab1* (Howell et al., 1997; Sheldon et al., 1997; Ware et al., 1997), *cdk5* (Ohshima et al., 1996), *p35* (Chae et al., 1997), and *filamin 1* (Fox et al., 1998), in addition to *LIS1* and *DCX*, have been found to

lead to specific phenotypes in which neuronal migration is disturbed. Two of these proteins (Reelin and mDab1) have been implicated as required for the proper arrest after completing migration to the cortex (Pearlman and Sheppard, 1996; Frotscher, 1997), whereas Filamin 1 appears to be required at the very onset of migration. In contrast, DCX, LIS1, and Cdk5/p35 may act during the ongoing process of migration. Cdk5/p35 has additional effects on neurite outgrowth (Nikolic et al., 1996) through interactions with the Rho GTPases (Nikolic et al., 1998) and thereby the actin cytoskeleton and has also been shown to phosphorylate the MAP tau (Kobayashi et al., 1993). Thus, neuronal migration to the cortex may be regulated by genetic mechanisms acting at the beginning of migration and the end of migration, and perhaps by one or more mechanisms during the process of migration. We speculate that, whereas actin-based mechanisms are particularly important to extending the leading process of the migrating neuron, microtubule-based mechanisms may regulate nucleokinesis.

Experimental Procedures

Cloning of the Murine Homolog of DCX

Murine *DCX* was cloned by RT-PCR using human primers and subsequently sequenced. Murine-specific PCR primers were then developed and used to confirm the murine *DCX* sequence (GenBank accession number 3641670). The murine and human full-length *DCX* both hybridized to a single 9.5 kb band on a murine Northern blot (Gleeson et al., 1998). For this reason, and because the human *DCX* homolog was available before the mouse homolog was cloned, the human homolog was used for in situ hybridization studies.

Overexpression of DCX

Full-length human *DCX* was cloned into the KpnI site of pcDNA3.1(+) (Invitrogen, Carlsbad, CA) and misexpressed in COS7 cells by transient transfection with Superfectamine (Qiagen, Chatsworth, CA), according to the manufacturer's recommendations. Cells were harvested 2 days later by adding boiling protein sample buffer (20 mM Tris, 5% glycerol, 0.625% SDS, 5% β-mercaptoethanol).

In Situ Hybridization

In situ hybridization was performed essentially as described (Wilkinson and Nieto, 1993) using 15 μm tissue sections from whole mouse embryos at E14, whole heads at E17, or brains at P0. Sections were permeated with 1 μg/ml proteinase K for 1 min, prehybridized at 70°C for 1 hr, and probed overnight with a digoxigenin-labeled RNA antisense or sense DCX probe at a final concentration of 1 μg/ml in hybridization solution at 70°C. Hybridization solution contained 50% formamide, 5× SSC, 50 μg/ml yeast tRNA, 1% SDS, and 50 μg/ml heparin. Sections were rinsed in PBT four times and immunolabeled with 1:2000 anti-digoxigen alkaline phosphatase overnight at 37°C. Sections were developed with NBT/X-phos (Boehringer Mannheim) overnight and mounted in Permount.

Generation of DCX-Specific Antisera

In order to generate antisera reactive to both human and mouse DCX protein, a 16-mer polypeptide corresponding to the DCX carboxyl terminus (Cys-YLPLSLDDSDSLGDSM-free acid) was conjugated to KLH for immunization (Covance, Denver, PA). α-DCX antisera was used directly at 1:2000 for Western analysis and 1:50 for immunofluorescence.

Western Analysis

Total protein was run on a 10% SDS-PAGE gel and probed with either α-DCX, α-pan MAP2 (1:500), or α-mDab1 (1:500) primary antibody and developed using an HRP anti-rabbit or anti-mouse secondary antibody (Biorad, Hercules, CA) at 1:3000 and ECL (Amersham, Arlington Heights, IL). Fifty micrograms of total protein were loaded for expression studies, and ~50% of the pellet was loaded for DCX microtubule experiments. Blots were stripped and probed for tubulin to control for protein loading.

Immunohistochemistry

Sections were prepared as for in situ hybridization, as above, and incubated overnight with primary antibodies in block. Sections were then rinsed with PBS and incubated with Cy3 or FITC-labeled secondary antibody (Jackson Labs, Bar Harbor, ME) (diluted 1:100), rinsed several times in PBS, mounted, and examined under an Olympus fluorescent microscope. Negative controls for DCX were run in parallel using preimmune sera as the primary antisera. Colabeling was done with monoclonal antibodies to TuJ1 (Research Diagnostics, Flanders, NJ), calbindin (Sigma Immunochemicals, St. Louis, MO), GFAP (Sigma Immunochemicals), TAG-1 (Developmental Hybridoma Studies Bank at the University of Iowa), and Reelin (G10 monoclonal) (gift of A. Goffinet), all at a 1:200 dilution.

Imprint Assay

Inprint assays were performed as previously described (Anton et al., 1996). Briefly, E17 mouse cortex was removed and sectioned at 75 μm, incubated in CMF-PBS with 10 U/ml papain for 10 min, then in MEM with 2 mg/ml ovomucoid inhibitor and 100 mg/ml DNAse for 10 min, washed in media, and placed overnight on glass coverslips that had been treated with Cell-Tak (Beckton Dickenson). The cortex was gently removed with excess media, and cortical imprints containing radial migration units were observed and fixed for subsequent immunofluorescence. Imprints were stained with DCX antisera and Rat-401 antibody (Developmental Studies Hybridoma Bank) and counterstained with DAPI.

Immunofluorescence of Cultured Neurons, Colchicine/Cytochalasin B Treatment, and Transfection of Primary Cortical Cultures

Primary cortical cells were harvested from E17 rats, dissociated in papain, plated at a density of 5×10^5/ml of culture media in MEM with 10% fetal calf serum, and cultured for 2 days on microwell poly-D-lysine-coated coverslips. Colchicine (Sigma) (10 μg/ml), cytochalasin B (Sigma) (5 μg/ml), or vehicle was added for 0–3 hr. Cells were rinsed briefly in K-PIPES (80 mM K-PIPES [pH 6.8], 5 mM EGTA, 2 mM $MgCl_2$); fixed in 0.5% glutaraldehyde with 0.1% Triton X-100; quenched in 1 mg/ml $NaBH_4$; blocked with 1% BSA, 0.25% saponin, and 5 mM lysine for 10 min; incubated with primary antibodies as above for 1 hr; rinsed extensively with K-PIPES and incubated with Cy3 or FITC-conjugated secondary antibody (diluted 1:50) for 1 hr; rinsed extensively in K-PIPES; and postfixed in 4% paraformaldehyde for 30 min. Nuclei were visualized using 1 μM TOTO-3 (Molecular Probes) for 30 min, rinsed in water, mounted in Aquamount, and examined using a Biorad 1100 confocal microscope. Transfection of cultures was performed as described (Xia et al., 1996). Briefly, a mixture of 132 μl of water, 15 μl of 2.5 M $CaCl_2$, and 30 μg of DNA was added to 150 ml of 2× HEPES-buffered saline and incubated for 30 min. Neuronal cultures were incubated for 3 days after plating, and the transfection mix was left on the cells for 45 min. Cultures were processed 2 days after transfection. Some transfected cells were treated with colchicine (10 μg/ml for 2 hr) prior to fixation and microtubule visualization (as above).

Isolation of Microtubules from Brain

Four grams of newborn rat brain was homogenized in MES buffer (100 mM MES [pH 6.6], 1 mM EGTA, 1 mM $MgSO_4$, and 25 mM NaF and benzamidine, leupeptin, pepstatin A, aprotinin, and AEBSF protease inhibitors) at 4°C. The homogenate was centrifuged at 25,000 RPM for 15 min in a Beckman Optima centrifuge in the TLA 100.3 rotor, and the supernatant was subsequently centrifuged similarly at 75,000 RPM for 90 min, giving a tubulin-rich supernatant. Half of the supernatant was treated with 10 μM taxol (Calbiochem) and 1 mM GTP and half was treated with only 1 mM GTP. Both fractions were incubated for 25 min at 37°C to allow microtubules to polymerize, added over 1 vol of a 10% sucrose/MES buffer in a centrifuge tube, and centrifuged at 25,000 RPM at 35°C for 30 min. The supernatant and microtubule pellet were boiled in sample buffer and analyzed by Western blot for the presence of DCX.

Microtubule Cycling

A crude microtubule preparation from calf brain was cycled twice through successive warm/cold exposure in PEM buffer (100 mM PIPES [pH 6.6], 1 mM EGTA, 1 mM $MgSO_4$) with 1 mM GTP. Subsequently, extract from COS cells overexpressing wild-type DCX was added to the microtubule pellet in order to keep the tubulin concentration above the critical concentration for polymerization. The mixture was then subjected to three cycles of cold depolymerization followed by warm polymerization (Vallee, 1986), with aliquots removed at each step for later Western analysis using anti-DCX and anti α-tubulin antibodies.

Microtubule Polymerization Assay

In order to generate recombinant protein, *DCX* was cloned into the NdeI sites of the pET21a+ (Novagen, Madison, WI) vector and protein produced in BL21 *E. coli* (Stratagene), according to the manufacturer's recommendations. Briefly, a single clone was grown until optical density (O. D.) 600 equaled 0.4–0.6 and was induced with 1 mM IPTG. After 2 hr, the pellet was resuspended in 1× binding buffer, sonicated, and cleared by centrifugation, and the supernatant was run on an equilibrated Ni^{2+} column. The column was washed with 10 vol of 1× binding buffer and 6 vol of 1× wash buffer and then eluted with 6 vol of 1× elution buffer, dialyzed overnight against 100 mM HEPES [pH 7.5], 200 mM NaCl, 10 mM $MgCl_2$ at 4°C, and concentrated to 5 mg/ml on a Centricon column (Amicon, Beverly, MA). Phosphocellulose-purified (PCP) tubulin (Cytoskeleton, Denver, CO) was added to 1 mg/ml, in 1 mM GTP, in PEM buffer. Just before sample analysis, either recombinant MAP2C (kindly provided by D. L. Purich, University of Florida, Gainseville), recombinant DCX, or vehicle was added and briefly mixed. The kinetics of the diffraction for each sample was measured by right angle scattering in a quartz cuvette with a transmitted wavelength of 340 nM and a detected wavelength of 345 nM at a 90° angle to the transmitted beam for 30 min at 37°C in a Perkin Elmer LS50B fluorimeter. The initial diffraction was set to zero at time zero for each sample. At the conclusion of the experiment, the samples were adhered to grids, negatively stained with uranyl acetate, and examined by electron microscopy to confirm that changes in diffraction represented microtubule formation. The mean width of microtubule bundles, either in the absence or presence of 70 μg/ml DCX, was determined by counting the number of tightly associated individual 25 nm fibers in four photomicrographs from each sample ($n > 100$).

Rhodamine-labeled tubulin (Cytoskeleton) was mixed 1:4 with PCP tubulin to a final concentration of 0.5 mg/ml, and DCX was added in BRB80 buffer (80 mM PIPES [pH 6.8], 1 mM $MgCl_2$, 1 mM EGTA) in 1 mM GTP in the presence of recombinant DCX from 0.7–0.01 mg/ml for 15 min at 37°C. Samples were fixed in BRB80 with 0.1% glutaraldehyde and 20% glycerol. An aliquot of the sample was visualized with fluorescent microscopy. Microtubule length in the absence or presence of 175 μg/ml DCX was determined by projecting slides of photographs obtained from each sample. Approximately 100 individual microtubules were scored in this fashion.

Acknowledgments

We wish to thank P. Allen, T. Chae, A. Chenn, J. Corbo, Y. Feng, M. Greenberg, P. Janmey, K. Kosik, T. Mayer, E. Olson, T. Mitchison, E. Monuki, R. Ratan, R. Segal, and M. Shirasu for helpful comments and discussions; Q. Lu for help performing in situ hybridization; R. Ratan for providing primary cortical neurons; A. M. Goffinet for anti-Reelin antibody; E. Olson for anti-mDab1 antibody; E. Anton for staining of radial migratory units; D. L. Purich for recombinant MAP2C; and P. Sheffield for assistance with DCX protein purification. This work was supported by grants from the NINDS (R01-NS 35129 and R01-NS 38097 to C. A. W., 5K12NS01701–04 to J. G. G.) and from the Howard Hughes Medical Institute Medical Student Research Training Program (P. T. L.) and by the Mental Retardation Research Center at Children's Hospital, Boston.

Received March 1, 1999; revised June 3, 1999.

References

Anton, E.S., Cameron, R.S., and Rakic, P. (1996). Role of neuron–glial junctional domain proteins in the maintenance and termination of neuronal migration across the embryonic cerebral wall. J. Neurosci. *16*, 2283–2293.

Baas, P.W., and Joshi, H.C. (1992). Gamma-tubulin distribution in the neuron: implications for the origins of neuritic microtubules. J. Cell Biol. *119*, 171–178.

Baas, P.W., Deitch, J.S., Black, M.M., and Banker, G.A. (1988). Polarity orientation of microtubules in hippocampal neurons: uniformity in the axon and nonuniformity in the dendrite. Proc. Natl. Acad. Sci. USA *85*, 8335–8339.

Berg, M.J., Schifitto, G., Powers, J.M., Martinez-Capolino, C., Fong, C.T., Myers, G.J., Epstein, L.G., and Walsh, C.A. (1998). X-linked female band heterotopia–male lissencephaly syndrome. Neurology *50*, 1143–1146.

Black, M.M., Cochran, J.M., and Kurdyla, J.T. (1984). Solubility properties of neuronal tubulin: evidence for labile and stable microtubules. Brain Res. *295*, 255–263.

Brunati, A.M., James, P., Guerra, B., Ruzzene, M., Donella-Deana, A., and Pinna, L.A. (1996). The spleen protein–tyrosine kinase TPK-IIB is highly similar to the catalytic domain of p72syk. Eur. J. Biochem. *240*, 400–407.

Chae, T., Kwon, Y.T., Bronson, R., Dikkes, P., Li, E., and Tsai, L.H. (1997). Mice lacking p35, a neuronal specific activator of Cdk5, display cortical lamination defects, seizures, and adult lethality. Neuron *18*, 29–42.

D'Arcangelo, G., Miao, G.G., Chen, S.C., Soares, H.D., Morgan, J.I., and Curran, T. (1995). A protein related to extracellular matrix proteins deleted in the mouse mutant reeler. Nature *374*, 719–723.

Denarier, E., Fourest-Lieuvin, A., Bosc, C., Pirollet, F., Chapel, A., Margolis, R.L., and Job, D. (1998). Nonneuronal isoforms of STOP protein are responsible for microtubule cold stability in mammalian fibroblasts. Proc. Natl. Acad. Sci. USA *95*, 6055–6060.

des Portes, V., Pinard, J.M., Billuart, P., Vinet, M.C., Koulakoff, A., Carrie, A., Gelot, A., Dupuis, E., Motte, J., Berwald-Netter, Y., et al. (1998). A novel CNS gene required for neuronal migration and involved in X-linked subcortical laminar heterotopia and lissencephaly syndrome. Cell *92*, 51–61.

Desai, A., and Mitchison, T.J. (1997). Microtubule polymerization dynamics. Annu. Rev. Cell Dev. Biol. *13*, 83–117.

Edmondson, J.C., and Hatten, M.E. (1987). Glial-guided granule neuron migration in vitro: a high-resolution time-lapse video microscopic study. J. Neurosci. *7*, 1928–1934.

Fox, J.W., Lamperti, E.D., Eksioglu, Y.Z., Hong, S.E., Feng, Y., Graham, D.A., Scheffer, I.E., Dobyns, W.B., Hirsch, B.A., Radtke, R.A., et al. (1998). Mutations in filamin 1 prevent migration of cerebral cortical neurons in human periventricular heterotopia. Neuron *21*, 1315–1325.

Frotscher, M. (1997). Dual role of Cajal-Retzius cells and reelin in cortical development. Cell Tissue Res. *290*, 315–322.

Furley, A.J., Morton, S.B., Manalo, D., Karagogeos, D., Dodd, J., and Jessell, T.M. (1990). The axonal glycoprotein TAG-1 is an immunoglobulin superfamily member with neurite outgrowth-promoting activity. Cell *61*, 157–170.

Gaskin, F., Cantor, C.R., and Shelanski, M.L. (1974). Turbidimetric studies of the in vitro assembly and disassembly of porcine neurotubules. J. Mol. Biol. *89*, 737–755.

Gleeson, J.G., and Walsh, C.A. (1997). New genetic insights into cerebral cortical development. In Normal and Abnormal Development of Cortex, A. Galaburda and E. Christen, eds. (Berlin: Springer-Verlag), pp. 145–163.

Gleeson, J.G., Allen, K.M., Fox, J.W., Lamperti, E.D., Berkovic, S., Scheffer, I., Cooper, E.C., Dobyns, W.B., Minnerath, S.R., Ross, M.H., and Walsh, C.A. (1998). doublecortin, a brain-specific gene mutated in human X-linked lissencephaly and double cortex syndrome, encodes a putative signaling protein. Cell *92*, 63–72.

Gleeson, J.G., Minnerath, S.R., Fox, J.W., Allen, K.M., Luo, R.F., Hong, S.E., Berg, M.J., Kuzniecky, R., Reitnauer, P.J., Borgatti, R.,

et al. (1999). Characterization of mutations in the gene doublecortin in patients with double cortex syndrome. Ann. Neurol. *45*, 146–153.

Gregory, W.A., Edmondson, J.C., Hatten, M.E., and Mason, C.A. (1988). Cytology and neuron–glial apposition of migrating cerebellar granule cells in vitro. J. Neurosci. *8*, 1728–1738.

Guillaud, L., Bosc, C., Fourest-Lieuvin, A., Denarier, E., Pirollet, F., Lafanechere, L., and Job, D. (1998). STOP proteins are responsible for the high degree of microtubule stabilization observed in neuronal cells. J. Cell Biol. *142*, 167–179.

Hatten, M.E., and Heintz, N. (1995). Mechanisms of neural patterning and specification in the developing cerebellum. Annu. Rev. Neurosci. *18*, 385–408.

Hattori, M., Adachi, H., Tsujimoto, M., Arai, H., and Inoue, K. (1994). Miller-Dieker lissencephaly gene encodes a subunit of brain platelet-activating factor acetylhydrolase. Nature *370*, 216–218.

Hockfield, S., and McKay, R.D.G. (1985). Identification of major cell classes in the developing mammalian nervous system. J. Neurosci. *5*, 3310–3328.

Howell, B.W., Hawkes, R., Soriano, P., and Cooper, J.A. (1997). Neuronal position in the developing brain is regulated by mouse disabled-1. Nature *389*, 733–737.

Julien, J.P., and Mushynski, W.E. (1998). Neurofilaments in health and disease. Prog. Nucleic Acids Res. Mol. Biol. *61*, 1–23.

Kaech, S., Ludin, B., and Matus, A. (1996). Cytoskeletal plasticity in cells expressing neuronal microtubule-associated proteins. Neuron *17*, 1189–1199.

Knops, J., Kosik, K.S., Lee, G., Pardee, J.D., Cohen-Gould, L., and McConlogue, L. (1991). Overexpression of tau in a nonneuronal cell induces long cellular processes. J. Cell Biol. *114*, 725–733.

Kobayashi, S., Ishiguro, K., Omori, A., Takamatsu, M., Arioka, M., Imahori, K., and Uchida, T. (1993). A cdc2-related kinase PSSALRE/cdk5 is homologous with the 30 kDa subunit of tau protein kinase II, a proline-directed protein kinase associated with microtubule. FEBS Lett. *335*, 171–175.

Liesi, P. (1992). Neuronal migration on laminin involves neuronal contact formation followed by nuclear movement inside a preformed process. Exp. Neurol. *117*, 103–113.

Lois, C., and Alvarez-Buylla, A. (1994). Long-distance migration in the adult mammalian brain. Science *264*, 1145–1148.

Lois, C., Garcia-Verdugo, J.M., and Alvarez-Buylla, A. (1996). Chain migration of neuronal precursors. Science *271*, 978–981.

Mareck, A., Fellous, A., Francon, J., and Nunez, J. (1980). Changes in composition and activity of microtubule-associated proteins during brain development. Nature *284*, 353–355.

Margolis, R.L., Rauch, C.T., and Job, D. (1986). Purification and assay of a 145-kDa protein (STOP145) with microtubule-stabilizing and motility behavior. Proc. Natl. Acad. Sci. USA *83*, 639–643.

Matsuo, N., Kawamoto, S., Matsubara, K., and Okubo, K. (1998). Cloning and developmental expression of the murine homolog of doublecortin. Biochem. Biophys. Res. Commun. *252*, 571–576.

Matus, A. (1988). Microtubule-associated proteins: their potential role in determining neuronal morphology. Annu. Rev. Neurosci. *11*, 29–44.

Matus, A., Bernhardt, R., Bodmer, R., and Alaimo, D. (1986). Microtubule-associated protein 2 and tubulin are differently distributed in the dendrites of developing neurons. Neuroscience *17*, 371–389.

Morris, J.R., and Lasek, R.J. (1982). Stable polymers of the axonal cytoskeleton: the axoplasmic ghost. J. Cell Biol. *92*, 192–198.

Morris, S.M., Albrecht, U., Reiner, O., Eichele, G., and Yu-Lee, L.Y. (1998). The lissencephaly gene product Lis1, a protein involved in neuronal migration, interacts with a nuclear movement protein, NudC. Curr. Biol. *8*, 603–606.

Nikolic, M., Dudek, H., Kwon, Y.T., Ramos, Y.F., and Tsai, L.H. (1996). The cdk5/p35 kinase is essential for neurite outgrowth during neuronal differentiation. Genes Dev. *10*, 816–825.

Nikolic, M., Chou, M.M., Lu, W., Mayer, B.J., and Tsai, L.H. (1998). The p35/Cdk5 kinase is a neuron-specific Rac effector that inhibits Pak1 activity. Nature *395*, 194–198.

Nordquist, D.T., Kozak, C.A., and Orr, H.T. (1988). cDNA cloning and characterization of three genes uniquely expressed in cerebellum by Purkinje neurons. J. Neurosci. *8*, 4780–4789.

Ogawa, M., Miyata, T., Nakajima, K., Yagyu, K., Seike, M., Ikenaka, K., Yamamoto, H., and Mikoshiba, K. (1995). The reeler gene-associated antigen on Cajal-Retzius neurons is a crucial molecule for laminar organization of cortical neurons. Neuron *14*, 899–912.

Ohshima, T., Ward, J.M., Huh, C.G., Longenecker, G., Veeranna, Pant, H.C., Brady, R.O., Martin, L.J., and Kulkarni, A.B. (1996). Targeted disruption of the cyclin-dependent kinase 5 gene results in abnormal corticogenesis, neuronal pathology and perinatal death. Proc. Natl. Acad. Sci. USA *93*, 11173–11178.

O'Rourke, N.A., Dailey, M.E., Smith, S.J., and McConnell, S.K. (1992). Diverse migratory pathways in the developing cerebral cortex. Science *258*, 299–302.

O'Rourke, N.A., Chenn, A., and McConnell, S.K. (1997). Postmitotic neurons migrate tangentially in the cortical ventricular zone. Development *124*, 997–1005.

Pearlman, A.L., and Sheppard, A.M. (1996). Extracellular matrix in early cortical development. Prog. Brain Res. *108*, 117–134.

Rakic, P., Knyihar-Csillik, E., and Csillik, B. (1996). Polarity of microtubule assemblies during neuronal cell migration. Proc. Natl. Acad. Sci. USA *93*, 9218–9222.

Reiner, O., Carrozzo, R., Shen, Y., Wehnert, M., Faustinella, F., Dobyns, W.B., Caskey, C.T., and Ledbetter, D.H. (1993). Isolation of a Miller-Dieker lissencephaly gene containing G protein beta-subunit-like repeats. Nature *364*, 717–721.

Rice, D.S., Sheldon, M., D'Arcangelo, G., Nakajima, K., Goldowitz, D., and Curran, T. (1998). Disabled-1 acts downstream of Reelin in a signaling pathway that controls laminar organization in the mammalian brain. Development *125*, 3719–3729.

Rivas, R.J., and Hatten, M.E. (1995). Motility and cytoskeletal organization of migrating cerebellar granule neurons. J. Neurosci. *15*, 981–989.

Sapir, T., Elbaum, M., and Reiner, O. (1997). Reduction of microtubule catastrophe events by LIS1, platelet-activating factor acetylhydrolase subunit. EMBO J. *16*, 6977–6984.

Sheldon, M., Rice, D.S., D'Arcangelo, G., Yoneshima, H., Nakajima, K., Mikoshiba, K., Howell, B.W., Cooper, J.A., Goldowitz, D., and Curran, T. (1997). Scrambler and yotari disrupt the disabled gene and produce a reeler-like phenotype in mice. Nature *389*, 730–733.

Sossey-Alaoui, K., Hartung, A.J., Guerrini, R., Manchester, D.K., Posar, A., Puche-Mira, A., Andermann, E., Dobyns, W.B., and Srivastava, A.K. (1998). Human doublecortin (DCX) and the homologous gene in mouse encode a putative Ca^{2+}-dependent signaling protein, which is mutated in human X-linked neuronal migration defects. Hum. Mol. Genet. *7*, 1327–1332.

Stottmann, R.W., and Rivas, R.J. (1998). Distribution of TAG-1 and synaptophysin in the developing cerebellar cortex: relationship to Purkinje cell dendritic development. J. Comp. Neurol. *395*, 121–135.

Sullivan, K.F. (1988). Structure and utilization of tubulin isotypes. Annu. Rev. Cell Biol. *4*, 687–716.

Takemura, R., Okabe, S., Umeyama, T., Kanai, Y., Cowan, N.J., and Hirokawa, N. (1992). Increased microtubule stability and alpha tubulin acetylation in cells transfected with microtubule-associated proteins MAP1B, MAP2 or tau. J. Cell Sci. *103*, 953–964.

Tint, I., Slaughter, T., Fischer, I., and Black, M.M. (1998). Acute inactivation of tau has no effect on dynamics of microtubules in growing axons of cultured sympathetic neurons. J. Neurosci. *18*, 8660–8673.

Vallee, R.B. (1986). Reversible assembly purification of microtubules without assembly promoting agents and further purification of tubulin, microtubule-associated proteins, and MAP fragments. Methods Enzymol. *134*, 89–104.

Ware, M.L., Fox, J.W., Gonzalez, J.L., Davis, N.M., Lambert de Rouvroit, C., Russo, C.J., Chua, S.C., Jr., Goffinet, A.M., and Walsh, C.A. (1997). Aberrant splicing of a mouse disabled homolog, mdab1, in the scrambler mouse. Neuron *19*, 239–249.

Webb, B.C., and Wilson, L. (1980). Cold-stable microtubules from brain. Biochemistry *19*, 1993–2001.

Wilkinson, D.G., and Nieto, M.A. (1993). Detection of messenger

RNA by in situ hybridization to tissue sections and whole mounts. Methods Enzymol. *225*, 361–373.

Xia, Z., Dudek, H., Miranti, C.K., and Greenberg, M.E. (1996). Calcium influx via the NMDA receptor induces immediate early gene transcription by a MAP kinase/ERK-dependent mechanism. J. Neurosci. *16*, 5425–5436.

Xiang, X., Beckwith, S.M., and Morris, N.R. (1994). Cytoplasmic dynein is involved in nuclear migration in Aspergillus nidulans. Proc. Natl. Acad. Sci. USA *91*, 2100–2104.

Xiang, X., Osmani, A.H., Osmani, S.A., Xin, M., and Morris, N.R. (1995). NudF, a nuclear migration gene in Aspergillus nidulans, is similar to the human LIS-1 gene required for neuronal migration. Mol. Biol. Cell *6*, 297–310.